

Oscillatory waves in inhomogeneous neural media

P. C. Bressloff¹, S. E. Folias¹, A. Prat² and Y-X Li²

¹*Department of Mathematics, University of Utah, Salt Lake City, UT 84112*

²*Departments of Mathematics and Zoology, University of British Columbia, Vancouver, BC, Canada V6T 1Z2*

(Dated: September 3, 2003)

In this Letter we show that an inhomogeneous input can induce wave propagation failure in an excitatory neural network due to the pinning of a stationary front or pulse solution. A subsequent reduction in the strength of the input can lead to a Hopf instability of the stationary solution resulting in breather-like oscillatory waves.

PACS numbers: 87.*, 05.45.-a, 05.45.Xt

A number of theoretical studies have established the occurrence of traveling fronts [1, 2] and traveling pulses [3–5] in one-dimensional excitatory neural networks modeled in terms of evolution equations of the form

$$\begin{aligned} \tau \frac{\partial u(x,t)}{\partial t} + u(x,t) &= \int_{-\infty}^{\infty} w(x|x') f(u(x',t)) dx' \\ &\quad - \beta v(x,t) + I(x) \\ \frac{1}{\varepsilon} \frac{\partial v(x,t)}{\partial t} + v(x,t) &= u(x,t) \end{aligned} \quad (1)$$

where $u(x,t)$ is a neural field that represents the local activity of a population of excitatory neurons at position $x \in \mathbb{R}$, $I(x)$ is an external input, τ is a synaptic time constant (assuming first-order or exponential synapses), $f(u)$ denotes an output firing rate function and $w(x|x')$ is the strength of connections from neurons at x' to neurons at x . The neural field $v(x,t)$ represents some form of negative feedback recovery mechanism such as spike frequency adaptation or synaptic depression, with β, ε determining the relative strength and rate of feedback. (One can also incorporate higher-order synaptic and dendritic processes by replacing $\tau \partial u / \partial t + u$ with a more general linear differential operator $\hat{L}u$). It has been established [5] that there is a direct link between the above model and experimental studies of wave propagation in cortical slices where synaptic inhibition is pharmacologically blocked [6–8]. Since there is strong vertical coupling between cortical layers, it is possible to treat a thin cortical slice as an effective one-dimensional medium. Analysis of the model provides valuable information regarding how the speed of a traveling wave, which is relatively straightforward to measure experimentally, depends on various features of the underlying cortical circuitry.

One of the basic assumptions in the analysis of traveling wave solutions of equation (1) is that the system is spatially homogeneous, that is, the external input $I(x)$ is independent of x and the synaptic weights depend only on the distance between pre-synaptic and post-synaptic cells, $w(x|x') = w(x-x')$ with w a monotonically decreasing function of cortical separation. It can then be established that waves are in the form of traveling fronts in the absence of any feedback, whereas traveling pulses tend to occur when there is significant feedback [5]. However, the

cortex is more realistically modeled as an inhomogeneous medium. For example, inhomogeneities in the synaptic weight distribution w are likely to arise due to the patchy nature of long-range horizontal connections in superficial layers of cortex [9]. Another important source of inhomogeneity arises from external inputs induced by sensory stimuli, which may be modeled in terms of a nonuniform input $I(x)$. In this Letter we show that for appropriate choices of input inhomogeneity, wave propagation failure can occur due to the pinning of a stationary front or pulse solution. More significantly, we find that these stationary solutions can undergo a Hopf instability at a critical input amplitude, below which an oscillatory back-and-forth pattern of wave propagation or “breather” is observed. Our analysis predicts that the Hopf frequency depends on the relative strength and rate of feedback, but is independent of the details of the weight distribution. We also show numerically how a secondary instability leads to the generation of traveling waves. Analogous breather-like solutions have been found in inhomogeneous reaction diffusion systems [10, 11] and in numerical simulations of a realistic model of fertilization calcium waves [12].

First, let us consider traveling front solutions of equation (1) in the case of zero input $I(x) = 0$ and homogeneous weights $w(x|x') = w(x-x')$. For mathematical convenience, we take $w(x) = (2d)^{-1} e^{-|x|/d}$ with $\int_{-\infty}^{\infty} w(y) dy = 1$. The time and length scales are fixed by setting $\tau = d = 1$; typical values for these parameters are $\tau = 10 \text{ msec}$ and $d = 1 \text{ mm}$. As a further simplification, let $f(u) = \Theta(u - \kappa)$ where Θ is the Heaviside step function and κ is a threshold. We then seek a traveling front solution of the form $u(x,t) = U(\xi)$, $\xi = x - ct$, $c > 0$, such that $U(0) = \kappa$, $U(\xi) < \kappa$ for $\xi > 0$ and $U(\xi) > \kappa$ for $\xi < 0$. The center of the wave is arbitrary due to the translation symmetry of the homogeneous system. Eliminating the variable $V(\xi) = v(x - ct)$ by differentiating equation (1) twice with respect to ξ , leads to the second order differential equation

$$\begin{aligned} -c^2 U''(\xi) + c[1 + \varepsilon] U'(\xi) - \varepsilon[1 + \beta] U(\xi) \\ = -c w(\xi) - \varepsilon W(\xi) \end{aligned} \quad (2)$$

where $'$ denotes differentiation with respect to ξ and $W(\xi) = \int_{-\infty}^{\infty} w(y) dy$. The boundary conditions are

$U(0) = \kappa$ and $U(\pm\infty) = U_{\pm}$. Here U_{\pm} are the homogeneous fixed point solutions $U_- = 1/1 + \beta, U_+ = 0$. It follows that a necessary condition for the existence of a front solution is $\kappa < U_-$. The speed of a traveling front solution (if it exists) can then be obtained by solving the boundary value problem in the domains $\xi \leq 0$ and $\xi \geq 0$ and matching the solutions at $\xi = 0$. This leads to the bifurcation scenarios shown in figure 1. Such bifurcations also occur when the Heaviside output function is replaced by a smooth sigmoid function, which can then be analyzed using perturbation methods, and for more general monotonically decreasing weight distributions w [13]. Note that the bifurcation of the stationary front shown in figure 1(a) is analogous to the front bifurcation studied in reaction-diffusion equations, also known as the nonequilibrium Ising-Bloch (NIB) transition [10, 14–16]. Front bifurcations are of general interest, since they form organizing centers for a variety of nontrivial dynamics including the formation of breathers in the presence of weak input inhomogeneities (see below).

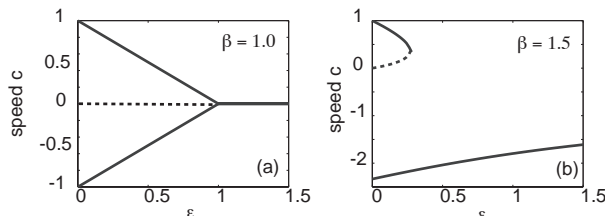


FIG. 1: Plot of wavefront speed c as a function of ε for fixed β and $\kappa = 0.25$. Stable (unstable) branches are shown as solid (dashed) curves. (a) If $2\kappa(1 + \beta) = 1$ then there exists a stationary front for all ε ; at a critical value of ε the stationary front loses stability and bifurcates into a left and a right moving wave (b) If $2\kappa(1 + \beta) > 1$ then there is a single left-moving wave for all ε and a pair of right-moving waves that annihilate in a saddle-node bifurcation. Left and right moving waves are reversed when $2\kappa(1 + \beta) < 1$ (not shown).

In the case of an inhomogeneous input, wave propagation failure can occur due to the formation of a stable stationary front solution. Stationary front solutions of equation (1) for homogeneous weights and $f(u) = \Theta(u - \kappa)$ satisfy the equation

$$(1 + \beta)U(x) = \int_{-\infty}^{x_0} w(x - x')dx' + I(x) \quad (3)$$

Suppose that $I(x)$ is a monotonically decreasing function of x . Since the system is no longer translation invariant, the position of the front is pinned to a particular location x_0 where $U(x_0) = \kappa$. Monotonicity of $I(x)$ ensures that $U(x) > \kappa$ for $x < x_0$ and $U(x) < \kappa$ for $x > x_0$. The center x_0 satisfies $(1 + \beta)\kappa = 1/2 + I(x_0)$, which implies that in contrast to the homogeneous case, there exists a stationary front over a range of threshold values (for fixed β); changing the threshold κ simply shifts the position

of the center x_0 . If the stationary front is stable then it will prevent wave propagation. Stability is determined by writing $u(x, t) = U(x) + p(x, t)$ and $v(x, t) = V(x) + q(x, t)$ and expanding equation (1) to first-order in (p, q) :

$$\begin{aligned} \frac{\partial p(x, t)}{\partial t} &= -p(x, t) - \beta q(x, t) \\ &\quad + \int_{-\infty}^{\infty} w(x - x')H'(U(x'))p(x', t)dx' \\ \frac{1}{\varepsilon} \frac{\partial q(x, t)}{\partial t} &= -q(x, t) + p(x, t) \end{aligned} \quad (4)$$

The spectrum of the associated linear operator is found by taking $p(x, t) = e^{\lambda t}p(x)$ and $q(x, t) = e^{\lambda t}q(x)$. Using the identity $H'(U(x) - \kappa) = \delta(x - x_0)/|U'(x_0)|$, we obtain the equation

$$(\lambda + 1)p(x) = \frac{w(x - x_0)}{|U'(x_0)|}p(x_0) - \frac{\varepsilon\beta p(x)}{\lambda + \varepsilon} \quad (5)$$

Equation (5) has two classes of solution. The first consists of any function $p(x)$ such that $p(x_0) = 0$, for which the corresponding eigenvalues always have negative real part. The second consists of solutions of the form $p(x) = Aw(x - x_0)$, $A \neq 0$, for which the corresponding eigenvalues are

$$\lambda_{\pm} = \frac{-\Lambda \pm \sqrt{\Lambda^2 - 4(1 - \Gamma)\varepsilon(1 + \beta)}}{2} \quad (6)$$

where

$$\Lambda = 1 + \varepsilon - (1 + \beta)\Gamma, \quad \Gamma = \frac{1}{1 + 2D} \quad (7)$$

with $D = |I'(x_0)|$. We have used the fact that $I'(x_0) \leq 0$ and $w(0) = 1/2$.

Equation (6) implies that the stationary front (if it exists) is locally stable provided that $\Lambda > 0$ or, equivalently, the gradient of the inhomogeneous input at x_0 satisfies

$$D > D_c \equiv \frac{1}{2} \frac{\beta - \varepsilon}{1 + \varepsilon} \quad (8)$$

Since $D \geq 0$, it follows that the front is stable when $\varepsilon > \beta$, that is, when the feedback is sufficiently weak or fast. On the other hand, if $\varepsilon < \beta$ then there is a Hopf bifurcation at the critical gradient $D = D_c$. Consider as an example the step inhomogeneity $I(x) = -(s/2) \tanh(\gamma x)$, where s is the size of the step and γ determines its steepness. A stationary front will exist provided that $s > \bar{s} \equiv |1 - 2\kappa(1 + \beta)|$. The gradient D depends on x_0 , which is itself dependent on β and κ . On eliminating x_0 , we can write $D = \gamma(s^2 - \bar{s}^2)/2s$. Substituting into equation (8) yields an expression for the critical value of s that determines the Hopf bifurcation points:

$$s_c = \frac{1}{2\gamma} \left[\frac{\beta - \varepsilon}{1 + \varepsilon} + \sqrt{\left(\frac{\beta - \varepsilon}{1 + \varepsilon}\right)^2 + 4\bar{s}^2\gamma^2} \right]. \quad (9)$$

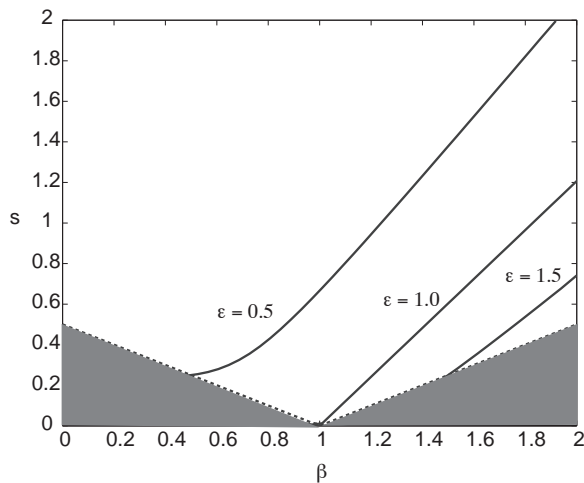


FIG. 2: Stability phase diagram for a stationary front in the case of a step input $I(x) = -s \tanh(\gamma x)/2$ where γ is the steepness of the step and s its height. Hopf bifurcation lines (solid curves) in $s - \beta$ parameter space are shown for various values of ε . In each case the stationary front is stable above the line and unstable below it. The shaded area denotes the region of parameter space where a stationary front solution does not exist. The threshold $\kappa = 0.25$ and $\gamma = 0.5$.

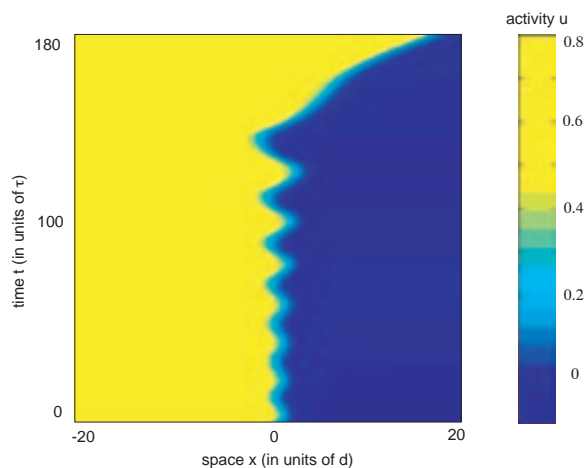


FIG. 3: Breather-like solution arising from a Hopf instability of a stationary front due to a slow reduction in the size s of a step input inhomogeneity and exponential weights. Here $\varepsilon = 0.5, \gamma = 0.5, \beta = 1, \kappa = 0.25$. The input amplitude $s = 2$ at $t = 0$ and $s = 0$ at $t = 180$. The amplitude of the oscillation steadily grows until it destabilizes at $s \approx 0.05$, leading to the generation of a traveling front.

The critical height s_c is plotted as a function of β for $\gamma = 0.5$ and various values of ε in Fig. 2. Note that close to the front bifurcation $\varepsilon = \beta$ a Hopf bifurcation occurs in the presence of a weak inhomogeneity. Numerically one finds that reducing the input amplitude below the critical point induces a transition to a breather-

like oscillatory front solution, whose frequency of oscillation is approximately equal to the critical Hopf frequency $\omega_H = \sqrt{\varepsilon(\beta - \varepsilon)}$. This suggests that the bifurcation is supercritical. Note that the frequency of oscillations only depends on the size and rate of the negative feedback, but is independent of the details of the synaptic weight distribution. As the input amplitude is further reduced, the breather itself becomes unstable and there is a secondary bifurcation to a traveling front. This is illustrated in Fig. 3, which shows a space-time plot of the developing breather as the input amplitude is slowly reduced.

The above analysis can be extended to the case of stationary pulse solutions in the presence of a unimodal input $I(x)$ which, for concreteness, is taken to be a Gaussian of width σ centered at the origin $I(x) = \mathcal{I}e^{-x^2/2\sigma^2}$. From symmetry arguments there exists a stationary pulse solution $U(x)$ of equation (1) centered at $x = 0$ with $U(\pm a/2) = \kappa$ and $U(\pm\infty) = 0$:

$$(1 + \beta)U(x) = \int_{-a/2}^{a/2} w(x - x')dx' + I(x) \quad (10)$$

The threshold κ and width a are related according to

$$(1 + \beta)\kappa = \left[I(a/2) + \frac{1 - e^{-a}}{2} \right] \equiv G(a) \quad (11)$$

Plotting the function $G(a)$ for a range of input amplitudes \mathcal{I} , it can be shown that for $\kappa(1 + \beta) < 0.5$ there exists a single pulse solution over the finite range of inputs $0 \leq \mathcal{I} \leq \kappa(1 + \beta)$, and no pulse solutions when $\mathcal{I} > \kappa(1 + \beta)$. On the other hand, when $\kappa(1 + \beta) > 0.5$ there exist two solution branches as illustrated in Fig. 4, one corresponding to a narrow pulse and the other to a broad pulse. These two branches coalesce at the critical point $\mathcal{I} = \mathcal{I}_{SN}$ where $G(a) = \kappa(1 + \beta)$ and $G'(a) = 0$.

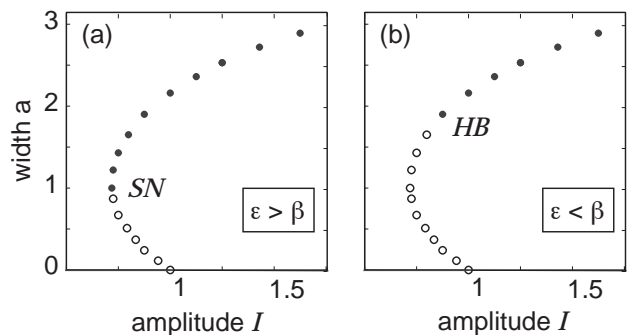


FIG. 4: Plot of pulse width a as a function of input amplitude \mathcal{I} obtained by numerically solving equation (11) for $\sigma = 1, \kappa = 0.5$ and $\beta = 1$. The lower branch is unstable whereas the upper branch is stable for large pulse width. (a) If $\varepsilon > \beta$ then the upper branch undergoes a saddle-node bifurcation at $\mathcal{I} = \mathcal{I}_{SN}$. (b) If $\varepsilon < \beta$ then the upper branch undergoes a Hopf bifurcation at $\mathcal{I} = \mathcal{I}_{HB} > \mathcal{I}_{SN}$.

Carrying out a linear stability analysis along similar lines to the case of a front leads to the following stability results [13]: (i) The single pulse solution for $\kappa(1+\beta) < 0.5$ is unstable. (ii) The lower branch of solutions (narrow pulse) for $\kappa(1+\beta) > 0.5$ is always unstable, whereas the upper branch (broad pulse) is stable for sufficiently large pulse width a . (iii) If $\varepsilon > \beta$ then the upper branch is stable for all $\mathcal{I} > \mathcal{I}_{SN}$ and undergoes a saddle node bifurcation at $\mathcal{I} = \mathcal{I}_{SN}$. (iv) If $\varepsilon < \beta$ then there exists a critical input amplitude \mathcal{I}_{HB} with $\mathcal{I}_{HB} > \mathcal{I}_{SN}$ such that the upper branch is stable for $\mathcal{I} > \mathcal{I}_{HB}$ and undergoes a Hopf bifurcation at $\mathcal{I} = \mathcal{I}_{HB}$. Numerically we find that the Hopf instability of the upper branch induces a breather-like oscillatory pulse solution as illustrated in Fig. 5. One finds that the associated Hopf frequency is again given by $\omega_H = \sqrt{\varepsilon(\beta - \varepsilon)}$, which is independent of the pulse-width a . For the parameter values used in Fig. 5, we have $\omega \approx 0.25\tau^{-1} = 25Hz$ assuming that $\tau = 10msec$. As the input amplitude \mathcal{I} is slowly reduced below \mathcal{I}_{HB} , the oscillations steadily grow until a new instability point is reached. Interestingly, the breather persists over a range of inputs beyond this secondary instability except that it now periodically emits pairs of traveling pulses. Furthermore, in this parameter regime we observe frequency-locking between the oscillations of the breather and the rate at which pairs of pulses are emitted from the breather. Note that although the homogeneous network ($\mathcal{I} = 0$) also supports the propagation of traveling pulses, it does not support the existence of a breather that can act as a source of these waves.

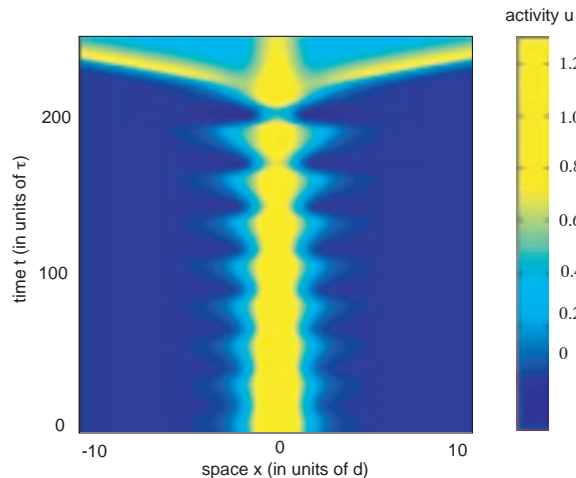


FIG. 5: Breather-like solution arising from a Hopf instability of a stationary pulse due to a slow reduction in the amplitude \mathcal{I} of a Gaussian input and exponential weights. Here $\mathcal{I} = 5.5$ at $t = 0$ and $\mathcal{I} = 1.5$ at $t = 250$. Other parameter values are $\varepsilon = 0.03, \beta = 2.5, \kappa = 0.3, \sigma = 1.0$. The amplitude of the oscillation steadily grows until it undergoes a secondary instability at $\mathcal{I} \approx 2$, beyond which the breather persists and periodically generates pairs of traveling pulses (only one of which is shown). The breather itself disappears when $\mathcal{I} \approx 1$.

Two major predictions of our analysis are (i) an inhomogeneous input current can induce oscillatory behavior in the form of breathing fronts and pulses and (ii) the oscillation frequency is approximately independent of the details of the underlying synaptic weight distribution, depending only on parameters that have a direct biological interpretation in terms of single cell recovery mechanisms. From an experimental perspective, our results could be tested by introducing an inhomogeneous current into a cortical slice and searching for these oscillations. One potential difficulty of such an experiment is that persistent currents tend to burn out neurons. In the case of traveling fronts, this might be avoided by operating the system close to the front bifurcation of the homogeneous network, see figure 1(a), such that only weak inhomogeneities would be needed to induce oscillations. An alternative approach might be to use some form of pharmacological manipulation of NMDA receptors, for example. Note that the usual method for inducing traveling waves in cortical slices (and in corresponding computational models) is to introduce short-lived current injections; once the wave is formed it propagates in a homogeneous medium (neglecting the modulatory effects of long-range horizontal connections [9]). In future work we will generalize our results to the case of a smooth output nonlinearity f and determine to what extent the oscillation frequency now depends on the form of the weight distribution w . We will also consider extensions to target waves in two-dimensional networks [13].

-
- [1] G. B. Ermentrout and J. B. Mcleod, Proc. Roy. Soc. Edin. A **123**, 461 (1993).
 - [2] M. A. P. Idiart and L. F. Abbott, Network **4**, 285 (1993).
 - [3] H. R. Wilson and J. D. Cowan, Kybernetik **13**, 55 (1973).
 - [4] S. Amari, Biol. Cybern. **27**, 77 (1977).
 - [5] D. Pinto and G. B. Ermentrout, SIAM J. Appl. Math **62**, 206 (2002).
 - [6] R. D. Chervin, P. A. Pierce, and B. W. Connors, J. Neurophysiol. **60**, 1695 (1988).
 - [7] D. Golomb and Y. Amitai, J. Neurophysiol. **78**, 1199 (1997).
 - [8] J.-Y. Wu, L. Guan, and Y. Tsau, J. Neurosci. **19**, 5005 (1999).
 - [9] P. C. Bressloff, Physica D **155**, 83 (2001).
 - [10] M. Bode, Physica D **106**, 270 (1997).
 - [11] A. Prat and Y.-X. Li (2003), submitted for publication.
 - [12] Y.-X. Li (2003), submitted for publication.
 - [13] S. E. Folias and P. C. Bressloff (2003), unpublished.
 - [14] J. Rinzel and D. Terman SIAM J. Appl. Math. **42**, 1111 (1982).
 - [15] A. Hagberg and E. Meron Nonlinearity **7**, 805 (1994).
 - [16] A. Hagberg and E. Meron and I. Rubinstein and B. Zaltman, Phys. Rev. Lett. **76**, 427 (1996).